Cooperation and competition of viscoelastic fluids and elastomeric microtubes subject to pulsatile forcing

Aimee M. Torres Rojas [*]
Departamento de Física y Química Teórica, Facultad de Química, Universidad Nacional Autónoma de México, Mexico City 04510, Mexico

E. Corvera Poiré [†]
Departamento de Física y Química Teórica, Facultad de Química, Universidad Nacional Autónoma de México, Mexico City 04510, Mexico and UBICS Institute of Complex Systems, Universitat de Barcelona, Martí i Franquès 1, Barcelona 08028, Spain

(Received 27 September 2019; accepted 2 June 2020; published 29 June 2020)

We analyze the dynamic behavior of viscoelastic fluids in elastic tubes subject to pulsatile pressure gradients. In particular, we study the dynamic permeability, a response function that relates linearly flow and pressure gradient in frequency domain. We have found resonances that can be associated to the elasticity of the tube and resonances that can be associated to the elasticity of the fluid. There is a rich phenomenology that includes cooperation and competition of both elasticities. Tuning of the system parameters allows for the excitation of the different modes in the system, sometimes giving responses that are larger than the ones of the corresponding systems with elasticity in only one of its elements. This behavior is similar to the one of two coupled oscillators. Our results are relevant for small confining geometries with low Young moduli. For example, for a microtube with a radius of a few hundred microns with the elasticity of polydimethylsiloxane (PDMS), in which a viscoelastic fluid, with the rheological parameters of blood, is driven by a pulsatile pressure gradient, resonance frequencies on the sound range are predicted. In a wide frequency range, the dynamic permeability is much lower than the one of the same fluid flowing in a poly(methyl methacrilate) (PMMA) tube. Our results are potentially useful for tailoring composite laboratory-on-a-chip devices, where introducing materials with different parameters in a device would induce an increase or decrease of the amplitude of the longitudinally averaged flow. We demonstrate that the magnitude of the dynamic permeability for a composite tube, at a given frequency of the driving pressure drop, determines the amplitude of the average flow along the composite tube.

DOI: 10.1103/PhysRevFluids.5.063303

I. INTRODUCTION

The dynamic permeability is the frequency-dependent fluid response to a dynamic pressure gradient. It relates pressure drop and flow and has information about which frequencies of the pressure drop could maximize or minimize the flow magnitude [1–6].

[*]Corresponding author: aimee.torres.rojas@gmail.com
[†]Corresponding author: eugenia.corvera@gmail.com

 ©2020 American Physical Society

Knowledge of the dynamic permeability of viscoelastic fluids might be relevant for biofluids, since these ones are generally viscoelastic, like blood, mucus, milk, and lymph [7,8]. Studying them in elastic confining media is important, since in natural systems biofluids are generally confined in elastic tubes, such as blood vessels, bronchia, milk ducts, or lymphatic vessels.

The study of the dynamics of viscoelastic fluids flowing in elastic media could also be relevant for laboratory-on-a-chip systems that test biofluids in elastomeric microdevices [9–11].

We have recently analyzed the dynamic behavior of Newtonian fluids in elastic tubes subject to pulsatile pressure gradients and showed that a resonant behavior at frequencies in the range of ultrasound emerges for fluids confined in elastomeric materials at microscales [12].

The effect that the elasticity of both the fluid and the confining media has on the dynamic permeability has only been considered to include the effect of longitudinally oscillating tubes in Maxwell fluids [13]. Other studies that have not considered the dynamic permeability have addressed the problem of flow induced by a wave traveling on the tube's wall for Maxwellian fluids [14,15].

In this paper, we consider a Maxwellian fluid, which is the most common model of viscoelasticity. We analyze the dynamic behavior of this fluid, subject to a pulsatile pressure gradient, flowing through an elastic tube that can have both axial and radial displacements of the wall. We show that the interplay between the elasticities of the fluid and the wall gives rise to resonances that could be roughly attributed to either the fluid or the wall. By moving the system parameters, one might tune one or the other to be the most relevant resonance of the system. These resonances are meaningful for small confining geometries with low Young moduli. For example, for a microtube of 200 mμ in diameter with the elasticity of polydimethylsiloxane (PDMS), in which a Maxwellian fluid with the rheological parameters of blood is driven by a pulsatile pressure gradient, resonance frequencies on the sound range are predicted. Our results are potentially useful for tailoring laboratory-on-a-chip devices, where changing the elasticity of different parts of a device, by the introduction of different materials, would change the dynamic permeability of the system. As a proof of concept, we analyze flow in a composite theoretical device made of two different materials, with the elastic properties of PDMS and poly(methyl methacrilate) (PMMA), and demonstrate that the magnitude of the dynamic permeability for a composite tube, which clearly differs from the one of a tube made of a single material, determines the amplitude of the longitudinally averaged flow along the composite tube.

II. MODEL EQUATIONS

We consider a tube whose radius, a, is much smaller than its length, l. We define x as the flow direction along the tube and r as the radial direction. We consider that the pressure in the radial direction adjust instantaneously at a given point along the flow direction, i.e., $\frac{\partial p}{\partial r} = 0$. So the system is subjected to a nonstationary pressure gradient which is a function of the direction along the flow and time, that is, $\nabla p(x,t) = \frac{\partial p(x,t)}{\partial x}\hat{\imath}$.

We consider conservation of mass and momentum for a linear Maxwellian incompressible fluid with density ρ, viscosity μ, and relaxation time t_r, for which convective terms are negligible. These equations are as follows:

$$\frac{\partial u}{\partial x} + \frac{1}{r}\frac{\partial (rv)}{\partial r} = 0, \tag{1}$$

$$t_r\,\rho\,\frac{\partial^2 u}{\partial t^2} + \rho\,\frac{\partial u}{\partial t} = -t_r\,\frac{\partial}{\partial t}\left(\frac{\partial p}{\partial x}\right) - \frac{\partial p}{\partial x} + \mu\left(\frac{\partial^2 u}{\partial r^2} + \frac{1}{r}\,\frac{\partial u}{\partial r}\right), \tag{2}$$

where $u(x,r,t)$ and $v(x,r,t)$ are the axial and radial velocities of the fluid, respectively.

We consider equations for the elastic motion of a tube with a thin thickness $h \ll a$, wall density ρ_w, Young modulus E, and Poisson ratio ν. Our equations allow for radial and axial displacements,

$\eta(x,t)$ and $\xi(x,t)$ [16,17],

$$\rho_w h \frac{\partial^2 \eta}{\partial t^2} = \sigma_{rr} - \frac{E h}{1-\nu^2}\left(\frac{\eta}{a^2} + \frac{\nu}{a}\frac{\partial \xi}{\partial x}\right), \tag{3}$$

$$\rho_w h \frac{\partial^2 \xi}{\partial t^2} = -\sigma_{rx} + \frac{E h}{1-\nu^2}\left(\frac{\partial^2 \xi}{\partial x^2} + \frac{\nu}{a}\frac{\partial \eta}{\partial x}\right). \tag{4}$$

The boundary conditions for stresses between the wall and the fluid imply that $\sigma_{rr} = p$ and $t_r \frac{\partial \sigma_{rx}}{\partial t} + \sigma_{rx} = \mu \frac{\partial u}{\partial r}|_a$, where the right-hand side of this equation has been considered at the mean position of the fluid-solid interface.

The continuity of velocities, in both the radial and axial directions between the fluid and the tube wall, approximated at the mean wall position, $r = a$, where the tube is neither expanded nor compressed, are given by

$$\frac{\partial \eta}{\partial t} = v\Big|_a; \quad \frac{\partial \xi}{\partial t} = u\Big|_a. \tag{5}$$

The approximation of boundary conditions, evaluated at $r = a$, substitutes a free boundary value problem by fixed boundary conditions, and is valid when the tube deformations, η and ξ, are much smaller than the average radius of the tube. It allows for an analytical treatment of the problem.

Solutions of Eqs. (1)–(5) are obtained using the methodology presented in Ref. [12]. We have considered the general form of stationary waves, i.e., waves that can be expressed as the product of a term dependent on the direction of propagation and a time-dependent term for pressure, fluid velocities, and wall displacements. Since stationary waves are characterized by having a dynamics with fixed values at certain points in space (nodes), this assumption allows us to impose fixed values of certain parameters at the system boundaries, for example, a constant value for pressure at the end of a finite tube (which is an experimental boundary condition commonly used in microfluidics). Solution of Eqs. (1)–(5), gives two equations for pressure and pressure gradient, in frequency domain, whose coefficients give a dispersion relation that relates the wave number of the propagating modes in terms of the frequency of the applied pressure gradient. Such equations are harmonic, that is,

$$\frac{\partial^2 \hat{p}(x,\omega)}{\partial x^2} = -k_a^2(A(\omega))\,\hat{p}(x,\omega) \tag{6}$$

and

$$\frac{\partial^3 \hat{p}(x,\omega)}{\partial x^3} = -k_b^2(A(\omega))\frac{\partial \hat{p}(x,\omega)}{\partial x}. \tag{7}$$

Consistency requires that $k_a^2 = k_b^2 = \kappa^2$. This gives a quadratic equation for $A(\omega)$ that is needed in order to know the solution of $u(x,r,t)$, $v(x,r,t)$, $\eta(x,t)$, and $\xi(x,t)$ in the frequency domain [18]. It is important to note that the wave number, $\kappa(\omega)$, gives the inverse of a characteristic length. Such characteristic length should be much larger than the tube radius for our solution to be valid. Since the analytical expression for κ, which is very complicated, involves all the system parameters, in practice, this condition has to be evaluated for the particular choice of fluid, confining elastic material, and geometrical confinement properties, that characterize our system.

The local axial velocity in frequency domain, $\hat{u}(x,r,\omega)$, in terms of the pressure gradient in frequency domain, $\frac{\partial \hat{p}(x,\omega)}{\partial x} = g(x)\hat{G}(\omega)$, is given by

$$\hat{u}(x,r,\omega) = -\frac{1}{\mu}\hat{K}^L(r,\omega)\,g(x)\hat{G}, \tag{8}$$

where

$$\hat{K}^L(r,\omega) = \left[\mu A(\omega) J_0(\delta r) - \frac{1}{\beta^2}\right], \tag{9}$$

$\delta = \sqrt{\frac{\rho}{\mu}(t_r\,\omega^2 + i\,\omega)}$, and $\beta = \sqrt{\frac{i\,\omega\,\rho}{\mu}}$. J_0 is the Bessel function of order zero, and $A(\omega)$ is the solution of a quadratic equation, given by $A(\omega) = \frac{-b \pm \sqrt{b^2 - 4\mathtt{a}c}}{2\mathtt{a}}$, where

$$\mathtt{a} = 2h\rho^2\omega^2\rho_w J_0(\delta a)\,F_1 + \frac{2\delta\mu\rho^2\omega J_1(\delta a)\,F_1}{\omega t_r + i},$$

$$b = ia\omega\rho\{2E\rho[\nu J_1(\delta a) - \delta a J_0(\delta a)] + h\delta\rho_w J_0(\delta a)F_2\} + \frac{\rho\,J_1(\delta a)[ia\mu\delta^2 + 2\omega h\rho_w(i\omega t_r - 1)]F_3}{\omega t_r + i} - \frac{2E\nu a\delta\rho\,[i\delta\mu J_1(\delta a) + \omega h\rho_w J_0(\delta a)(i\omega t_r - 1)]}{\omega t_r + i}$$

and

$$c = -Ea^2\delta\rho(\nu - 2) + \frac{ia\delta h\rho_w(i\omega t_r - 1)F_2}{\omega t_r + i}.$$

In these expressions, F_1, F_2, and F_3 are given by

$$F_1 = [a^2\omega^2\rho_w(\nu^2 - 1) + E]J_1(\delta a) - E\nu\delta a J_0(\delta a),$$
$$F_2 = a^2\omega^2\rho_w(\nu^2 - 1) - 2E\nu + E,$$
$$F_3 = a^2\omega^2\rho_w(\nu^2 - 1) + E.$$

Equation (8) can be averaged over the cross sectional area to give

$$\langle\hat{u}(x,\omega)\rangle_r = -\frac{1}{\mu}\hat{K}(\omega)\,g(x)\,\hat{G}, \tag{10}$$

where $\hat{K}(\omega)$ is a dynamic permeability of the form

$$\hat{K}(\omega) = \left[\mu\,A(\omega)\,\frac{2\,J_1(\delta\,a)}{\delta\,a} - \frac{1}{\beta^2}\right]. \tag{11}$$

Here J_1 is the Bessel function of order one. Equation (10) is a generalized Darcy's law for Maxwellian fluids flowing in elastic tubes. It relates locally—at each point, x, along the flow direction—the radially averaged velocity and the pressure gradient in the frequency domain. In the time domain, it relates locally the magnitude of the radially averaged velocity and the pressure gradient. In the limit of rigid vessels, it reduces to the dynamic permeability reported in Refs. [2,3].

We approximate the fluid flow along the flow direction, $Q(x,t)$, as the product of the average cross-sectional area of the tube, $\mathbb{A} = \pi a^2$, times the radially averaged axial velocity, i.e., $Q(x,t) \approx \mathbb{A}\,\langle u(x,t)\rangle_r$. Using Eq. (10), we can write flow in frequency domain as

$$\hat{Q}(x,\omega) = -\frac{\mathbb{A}\,\hat{K}(\omega)}{\mu}\,\frac{\partial\hat{p}}{\partial x}(x,\omega), \tag{12}$$

where $\frac{\partial\hat{p}}{\partial x}(x,\omega)$ is obtained from the solution of harmonic Eqs. (6) and (7) and is written in terms of the inlet pressure, $\hat{p}_i$, the outlet pressure, $\hat{p}_o$, and the tube's length, l, i.e.,

$$\frac{\partial\hat{p}}{\partial x}(x,\omega) = -\kappa\,\hat{p}_i\sin(\kappa\,x) + \kappa\,\frac{\hat{p}_o - \hat{p}_i\cos(\kappa\,l)}{\sin(\kappa\,l)}\cos(\kappa\,x). \tag{13}$$

Since the pressure gradient is different for different points along the flow direction, in practice Eq. (12) is of little use, since experimentally, one would, in general, not know the pressure gradient

at each point of the system. However, if one averages Eq. (12) along the flow direction, one obtains an interesting result, namely

$$\langle \hat{Q}(\omega) \rangle_x \equiv -\frac{\mathbb{A}\,\hat{K}(\omega)}{\mu} \left\langle \frac{\partial \hat{p}}{\partial x}(\omega) \right\rangle_x = -\frac{\mathbb{A}\,\hat{K}(\omega)}{\mu} \frac{\Delta \hat{p}}{l}. \tag{14}$$

This expression, for elastic tubes, conserves mathematically the same form than a generalized Darcy's law in frequency domain for rigid tubes, except that now *flow* means averaged flow along the flow direction, and the averaged pressure gradient is nothing else than the total pressure drop along the tube, namely, pressure at the outlet minus pressure at the inlet, divided by the tube's length. The dynamic permeability, $\hat{K}(\omega)$, conserves its meaning; namely, it is a measurement of the resistance to flow for each of the modes involved in the total pressure drop. When known as a function of frequency, it will tell us at which frequencies the amplitude of the longitudinally averaged flow is maximized (or minimized) [19].

In order to use Eq. (14), we first need to know Δp in time domain; this one can have any desired form, containing many modes, including a steady component. We then should transform it to frequency domain, to obtain $\Delta \hat{p}$, that can be used in Eq. (14), to obtain flow in frequency domain, $\langle \hat{Q}(\omega) \rangle_x$. Finally, we have to inverse Fourier transform this one to obtain flow in time domain, $\langle Q(t) \rangle_x$. For instance, for a single-mode pressure drop, $\Delta p(t) = -\Delta p_0 \cos(\omega_0 t)$, we can obtain the flow as a function of time (averaged along the x direction), i.e.,

$$\langle Q(t) \rangle_x = \frac{\mathbb{A}}{\mu} |\hat{K}(\omega_0)| \cos(\phi(\omega_0) - \omega_0 t) \frac{\Delta p_0}{l}, \tag{15}$$

where $|\hat{K}(\omega_0)|$ and $\phi(\omega_0)$ are the magnitude and phase of the dynamic permeability at the frequency imposed by the pressure drop. Note that $\phi(\omega_0)$ determines also the phase difference between flow and pressure drop [20]. From this equation, it becomes evident that the magnitude of the permeability is linearly related to the maximum amplitude of the longitudinally averaged flow.

III. RELEVANT CHARACTERISTIC FREQUENCIES

There are several characteristic frequencies in our system: On the one hand, we have the frequency characteristic of the viscous fluid, ω_μ,

$$\omega_\mu = 2\pi \frac{\mu}{\rho\, a^2}. \tag{16}$$

We then have the frequencies characteristic of the elastic wall, namely ω_e and ω_w, given by

$$\omega_e = 2\pi \frac{1}{a} \sqrt{\frac{E}{(1-\nu^2)\rho_w}} \tag{17}$$

and

$$\omega_w = 2\pi \frac{\mu}{\rho_w\, h\, a}. \tag{18}$$

The viscoelasticity of the fluid involves another characteristic frequency,

$$\omega_{t_r} = \frac{2\pi}{t_r}. \tag{19}$$

All these frequencies appear in the dimensionless form of the equations shown in the Appendix, as dimensionless characteristic frequencies of the form ω_μ/ω_e, ω_w/ω_e, and ω_μ/ω_{t_r}. For the case in which $\rho_w \approx \rho$, ω_w is proportional to ω_μ, and the first two dimensionless characteristic frequencies are not independent. The third dimensionless characteristic frequency is the inverse of the Deborah number, usually used for viscoelastic fluids.

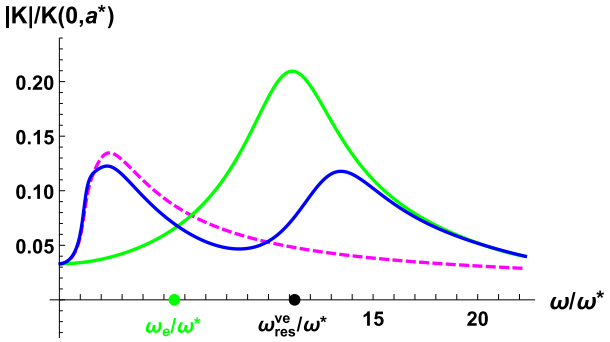

FIG. 1. Magnitude of the dynamic permeability as a function of frequency for three systems: viscoelastic fluid in an elastic tube (blue [dark solid] line), Newtonian fluid in an elastic tube (pink [light dashed] line), and viscoelastic fluid in a rigid tube (green [light solid] line). Parameters have been chosen to show the resonances of the three systems on the same figure. For the elastic tube: $E = 5\,\mathrm{Pa}$, $\rho_w = 5 \times 10^4\,\mathrm{kg/m^3}$, $\nu = 0.5$, and $h = 1\,\mu\mathrm{m}$. For the fluid: $\rho = 1050\,\mathrm{kg/m^3}$, $\mu = 4 \times 10^{-3}\,\mathrm{kg/m\,s}$, $t_r = 1 \times 10^{-3}$ s (in the viscoelastic case), and $t_r = 0$ s (in the Newtonian case). The radius was chosen as $a = 6 \times 10^{-5}$ m. Values of a^* and ω^*, for the parameters used in this figure, are 3.3×10^{-4} m and 220 rad/s, respectively.

In Ref. [12], we have found that Newtonian fluids flowing in elastic tubes have a resonance frequency, ω^N_{res}, whose behavior as a function of the tube's radius follows the one of the slowest mode among ω_e and ω_μ. When $\omega_\mu = \omega_e$, we can define a crossover frequency

$$\omega^* = \frac{\rho}{\rho_w}\frac{E}{\mu(1-\nu^2)}.$$

This happens for a particular value of the radius $a^* = \frac{\mu}{\rho}\sqrt{\frac{(1-\nu^2)\rho_w}{E}}$, which is an intrinsic length scale of the system. We use these quantities to normalize the figures' axes. Note that ω^* implies the particular value 1 of the dimensionless characteristic frequency ω_μ/ω_e.

On the other hand, there is an analytical expression [21] for Maxwellian fluids flowing in rigid tubes that approximates reasonably well the resonance frequency of this system in a wide range of tube radii, namely,

$$\omega^{ve}_{\mathrm{res}} = \frac{2.4048}{2\pi}\left[\omega_\mu \omega_{t_r}\right]^{1/2}. \tag{20}$$

IV. AN INTERPLAY OF TWO ELASTICITIES

We study a system with elasticity both in the fluid and in the tube. We find a response function that has two maxima at small frequencies, one around the resonance of a viscoelastic fluid in a rigid tube and one around the resonance of a Newtonian fluid in an elastic tube, a behavior similar to the behavior of coupled forced oscillators.

Figure 1 shows the dynamic permeability as a function of frequency for a viscoelastic fluid flowing in an elastic tube (blue [dark solid] line). We also show the dynamic permeability of a Newtonian fluid in an elastic tube (pink [light dashed] line) and the dynamic permeability of a viscoelastic fluid in a rigid tube (green [light solid] line). These two are used as reference systems in order to analyze our results. In the figure, we have chosen parameters that display two maxima with similar values of the dynamic permeability, one close to the resonance frequency of a Newtonian fluid in an elastic tube and another one close to the first resonance frequency of a Maxwellian fluid in a rigid tube (viscoelastic fluids always have several resonances at high frequencies).

Figure 2 shows how these maxima change when the wall density varies. In these curves, it becomes clear that, as the wall density increases, the first maximum coincides with the one of the

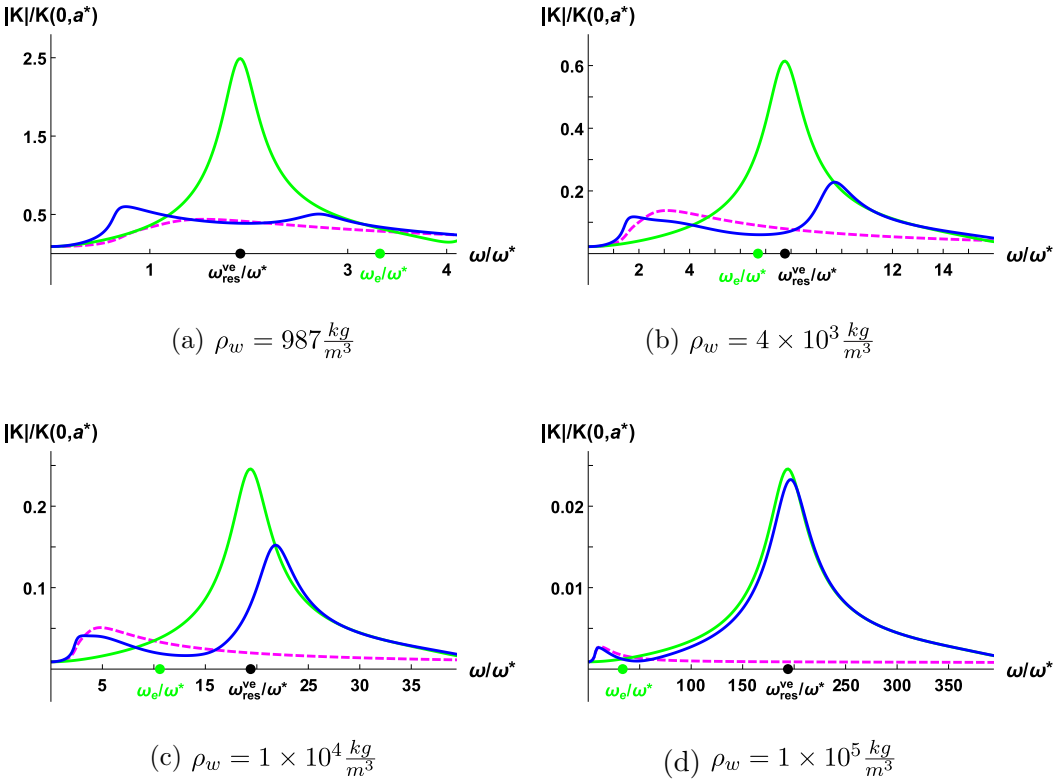

(a) $\rho_w = 987 \frac{kg}{m^3}$ (b) $\rho_w = 4 \times 10^3 \frac{kg}{m^3}$

(c) $\rho_w = 1 \times 10^4 \frac{kg}{m^3}$ (d) $\rho_w = 1 \times 10^5 \frac{kg}{m^3}$

FIG. 2. Magnitude of the dynamic permeability as a function of frequency for different values of the wall density and three different systems: viscoelastic fluid in an elastic tube (blue [dark solid] lines), Newtonian fluid in an elastic tube (pink [light dashed] lines), and viscoelastic fluid in a rigid tube (green [light solid] lines). For the elastic tube, $E = 1.0 \times 10^4$ Pa, $\nu = 0.5$, and $h = 10\,\mu$m. For the fluid, $\rho = 818\,\mathrm{kg/m^3}$, $\mu = 1\,\mathrm{kg/m\,s}$, and $t_r = 4 \times 10^{-5}$ s (in the viscoelastic case) and $t_r = 0$ s (in the Newtonian case). The radius was chosen as $a = 1 \times 10^{-4}$ m. For the first three figures, wall densities correspond to realistic materials. For figure (d), the density is too large to be realistic; it was chosen to illustrate how each of the maxima coincide with the ones of elasticity in only one of the system's elements. Values of a^* and ω^* for these figures are, respectively, (a) 3.3×10^{-4} m and 69431 rad/s; (b) 6.7×10^{-4} m and 17132 rad/s; (c) 1.1×10^{-3} m and 6853 rad/s; and (d) 3.3×10^{-3} m and 685 rad/s.

system that has elasticity only in the wall, while the second maximum coincides with the one of the system that has elasticity only in the fluid. In the mathematical limit in which the wall density tends to infinity, $\rho_w \to \infty$, which does not correspond to any physical density, the dynamic permeability of a Maxwell fluid in an elastic tube coincides exactly with the one of the Maxwell fluid in a rigid tube.

Figure 3 shows the permeability for the same three systems described in Fig. 2 for different tubes' radii. As we can see, for the range of radii in which resonances appear, increasing the tube radius enhances the effect of the wall's elasticity. For very large radii though, both resonances disappear [see Fig. 3(f)] but the resonance attributed to the fluid viscoelasticity disappears at smaller radii than the resonance due to the wall elasticity [see Figs. 3(c)–3(e)], where the second maxima has disappeared. As explained in Ref. [12], the resonance due to the wall's elasticity disappears because the steady-state permeability (for $\omega \to 0$) increases more quickly, with increasing radius, than the permeability at resonance, in such a way that it hinders the resonance. This feature makes this resonance typical of small elastic systems.

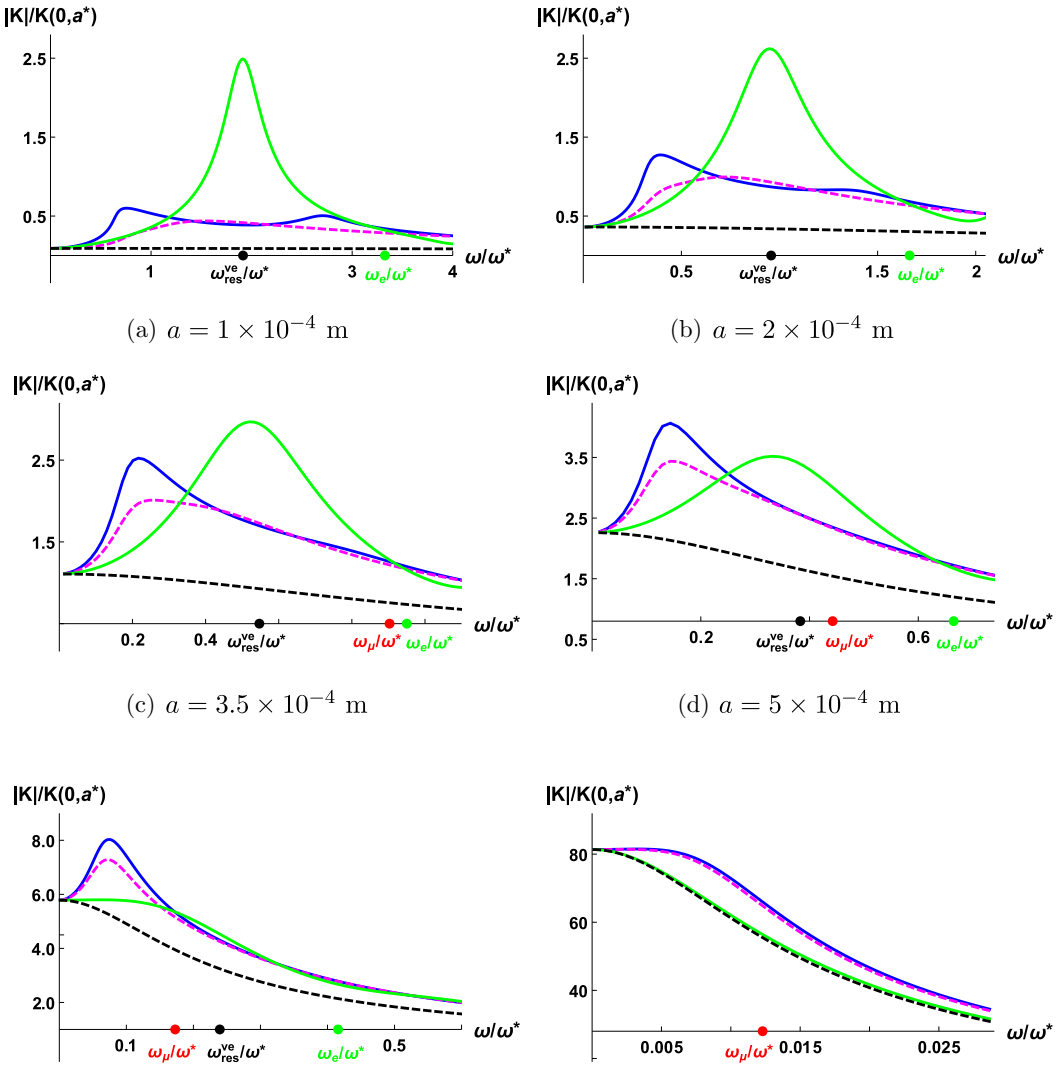

(a) $a = 1 \times 10^{-4}$ m

(b) $a = 2 \times 10^{-4}$ m

(c) $a = 3.5 \times 10^{-4}$ m

(d) $a = 5 \times 10^{-4}$ m

(e) $a = 8 \times 10^{-4}$ m

(f) $a = 3 \times 10^{-3}$ m

FIG. 3. Magnitude of the dynamic permeability as a function of frequency for different radii and four different systems: viscoelastic fluid in an elastic tube (blue [dark solid] lines), Newtonian fluid in an elastic tube (pink [light dashed] lines), viscoelastic fluid in a rigid tube (green [light solid] lines), and Newtonian fluid in a rigid tube (black dashed line). For the elastic tube, $\rho_w = 987\,\mathrm{kg/m^3}$, $E = 1.0 \times 10^4$ Pa, $\nu = 0.5$, and $h = 10\,\mu$m. For the fluid, $\rho = 818\,\mathrm{kg/m^3}$, $\mu = 1\,\mathrm{kg/m\,s}$, $t_r = 4 \times 10^{-5}$ s (in the viscoelastic case), and $t_r = 0$ s (in the Newtonian case). Values of a^* and ω^*, for the parameters used in this figure, are 3.3×10^{-4} m and 69431 rad/s, respectively.

Associating one maximum to the wall's elasticity and another one to the fluid viscoelasticity is only a convenient way of studying the system. Figure 3(c) shows that the maximum associated to the fluid elasticity has disappeared and nevertheless the height of the first maximum is much larger that the one of a Newtonian fluid in an elastic tube. We could therefore say that there are regimes in which one of the elasticities dominate the system, while there are others in which both elasticities cooperate to have a larger (or lower) response than they would have if only one of them were present.

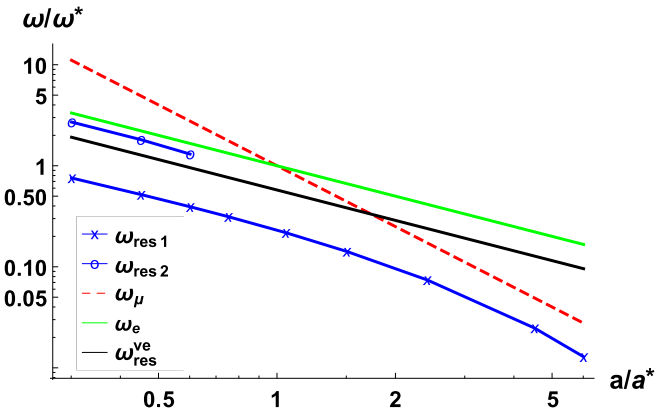

FIG. 4. Two resonance frequencies for viscoelastic fluid in an elastic tube, obtained from blue line in Fig. 3. The low resonance frequency, $\omega_{\text{res}\,1}$, associated to the elasticity of the tube, is marked by crosses. The high resonance frequency, $\omega_{\text{res}\,2}$, associated to the viscoelasticity of the fluid, is marked by circles. Red (dark dashed), green (light solid), and black (dark solid) lines, used as reference, indicate the characteristic frequencies of the system, given by Eqs. (16), (17), and (20), respectively.

For instance, the low-frequency range between 0 and 0.35, in the normalized frequency scale of Fig. 3(c), shows that the system has a larger response than the two reference systems in which only one of the elasticities is present. As a counter example, Fig. 1 shows a normalized frequency range between 6.3 and 9.8, in which the system permeability is smaller than the one of the Newtonian fluid in an elastic tube and much smaller than the one of a viscoelastic fluid in a rigid tube. A different situation is illustrated in Figs. 2(a)–2(d), where the dynamic permeability is between the ones of the systems in which only one of the elasticities is present, around the frequency range in which the second maximum occurs.

It is important to note that a system with elasticity in the fluid, in the tube, or in both has always a larger (or equal) permeability than a system in which no elasticity is present. This can be appreciated in Fig. 3 by noticing that any of the colored (dark solid, light dashed, and light solid) curves that have elasticity are above (or at) the black dashed line that corresponds to the permeability of a Newtonian fluid in a rigid tube.

It is also important to note that at large radii, once all the resonances have disappeared, the dynamic permeability of fluids (either Newtonian or viscoelastic) in elastic tubes is larger than the one of the same fluids confined in rigid tubes. This can be appreciated in Fig. 3(f).

Figure 4 displays the first two resonances of the system together with the characteristic frequencies given in Eqs. (16), (17), and (20). The low resonance frequency, $\omega_{\text{res}\,1}$, roughly associated to the tube, follows, as expected, the exponent of the elastic wall characteristic frequency [Eq. (17)] for small radii, and the exponent of the viscous characteristic frequency [Eq. (16)] for large radii. The high resonance frequency, $\omega_{\text{res}\,2}$, roughly associated to the fluid, follows, as expected, the exponent of the viscoelastic frequency given by Eq. (20).

Even though our paper emphasizes the cooperation and competition of both elasticities, we could ask what would happen if one changed the viscoelasticity of the fluid in an elastic tube. We would expect results to give similar tendencies as the ones obtained for viscoelastic fluids in rigid tubes. For instance, if we were to increase the viscoelasticity of the fluid, by increasing the fluid relaxation time, we would expect the maximum "due to the fluid" to move to smaller frequencies and the corresponding value of the dynamic permeability to be higher than at smaller relaxation times, as it happens in the rigid case. Figure 5 shows, for example, the equivalent of Fig. 2(b), for which dashed lines have been used for the larger relaxation time, confirming that the maximum "due to the fluid" behaves qualitatively as it does in the rigid case.

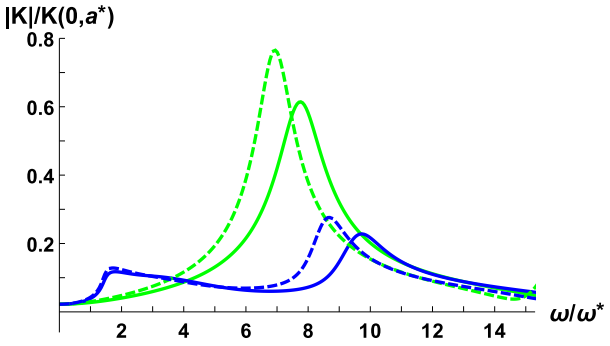

FIG. 5. Effect of different relaxation times in the dynamic permeability. Magnitude of the dynamic permeability as a function of frequency for two different fluid systems with different relaxation times: viscoelastic fluid with t_r^1 in an elastic tube (blue [dark] solid line), viscoelastic fluid with t_r^1 in a rigid tube (green [light] solid line), viscoelastic fluid with $t_r^2 > t_r^1$ in an elastic tube (blue [dark] dashed line), and viscoelastic fluid with $t_r^2 > t_r^1$ in a rigid tube (green [light] dashed line). The two values of the relaxation time used were $t_r^1 = 4 \times 10^{-5}$ s (solid lines) and $t_r^2 = 5 \times 10^{-5}$ s (dashed lines), corresponding to $\omega_{t_r}/\omega_\mu = 0.20$ and $\omega_{t_r}/\omega_\mu = 0.16$; and $t_r\omega^* = 0.69$ and $t_r\omega^* = 0.86$, respectively. The rest of the parameters are as in Fig. 2(b).

V. PROOF OF CONCEPT

Our results are potentially useful for tailoring composite laboratory-on-a-chip devices, where changing the elasticity of different parts of a device, by the introduction of different materials, would induce an increase or decrease of the amplitude of the longitudinally averaged flow at a given frequency. As a proof of concept, we analyze flow in a theoretical composite device made of two different materials and show that the magnitude of the dynamic permeability for a composite tube, at the driving frequency, determines the amplitude of the longitudinally averaged flow.

We now consider a tube of constant cross-sectional area, $\mathbb{A}$, composed of two different materials. For simplicity, we talk about the first part of the tube as "tube 1", that has length l_1, and the second part of the tube as "tube 2", that has length l_2. Flow conservation at the junction implies that outflow of tube 1 is equal to the inflow of tube 2, that is, $\hat{q}_1(x = l_1) = \hat{q}_2(x = 0)$, where $\hat{q}_1$ is the flow in tube 1 and $\hat{q}_2$ is the flow in tube 2. For tube 1, the inlet pressure is the inlet pressure of the system, $\hat{p}_{\text{in}}$, and the pressure at the exit is an unknown pressure at the junction, $\hat{p}_J$. For tube 2, the pressure at the entrance is the pressure at the junction, $\hat{p}_J$, and the pressure at the outlet is the output pressure of the system, $\hat{p}_{\text{out}}$. Using Eq. (12), for each of the tube's parts, in the equation for flow conservation at the junction, we can write an expression for the pressure at the junction, $\hat{p}_J$, as

$$\hat{p}_J = \frac{K_2\kappa_2 \sin(\kappa_1 l_1)\hat{p}_{\text{out}} + K_1\kappa_1 \sin(\kappa_2 l_2)\hat{p}_{\text{in}}}{K_1\kappa_1 \sin(\kappa_2 l_2)\cos(\kappa_1 l_1) + K_2\kappa_2 \sin(\kappa_1 l_1)\cos(\kappa_2 l_2)}, \tag{21}$$

where K_i and κ_i for $i = 1, 2$ are the dynamic permeability and the constant κ, appearing after Eq. (7), for each of the tube's parts, respectively.

On the other hand, the average flow along the composite tube is

$$\langle \hat{Q}_{\text{composite}} \rangle_x = \frac{l_1 \langle \hat{q}_1 \rangle_x + l_2 \langle \hat{q}_2 \rangle_x}{l_1 + l_2}, \tag{22}$$

which, using Eq. (14) to write $\langle \hat{q}_1 \rangle_x$ and $\langle \hat{q}_2 \rangle_x$, can be written as

$$\langle \hat{Q}_{\text{composite}} \rangle_x = -\mathbb{A}\frac{(K_2\hat{p}_{\text{out}} - K_1\hat{p}_{\text{in}})}{\mu(l_1 + l_2)} - \mathbb{A}\frac{(K_1 - K_2)}{\mu(l_1 + l_2)}\hat{p}_J, \tag{23}$$

with $\hat{p}_J$ given by Eq. (21).

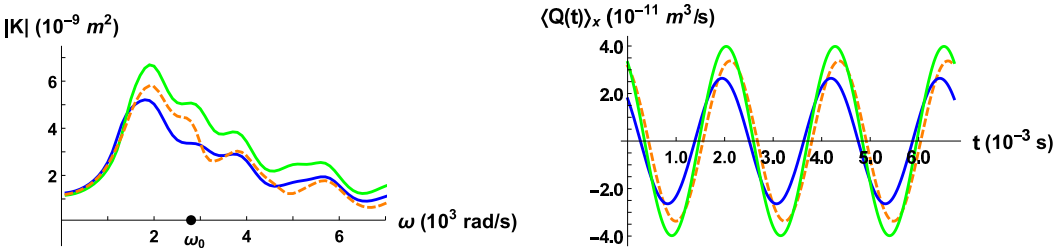

(a) (b)

FIG. 6. (a) Orange (light dashed) line is the magnitude of the dynamic permeability of a composite tube of total length of 2 cm in which the first third of the tube has the elastic properties of PDMS and the rest of the tube has the elastic properties of PMMA. As reference, the permeabilities of a tube made solely of PDMS and a tube made solely of PMMA are shown in blue (dark solid) and green (light solid) lines, respectively. (b) Average flow, along the flow direction, as a function of time for the three systems, with the same color coding used in panel (a), when the fluid is driven with an oscillatory pressure drop $\Delta p(t) = -\Delta p_0 \cos(\omega_0 t)$, with $\omega_0 = 2800$ rad/s and $\Delta p_0 = 20\,\text{Pa}$. Fluid parameters were chosen as $\rho = 1050\,\text{kg/m}^3$, $\mu = 4 \times 10^{-3}\,\text{kg/m s}$, and $t_r = 1 \times 10^{-3}$ s, which gives a Deborah number $\frac{\omega_{t_r}}{\omega_\mu} = 2.6$. For the driving frequency, ω_0, the Womersley number is $\sqrt{\frac{\omega_0}{\omega_\mu}} = 1.1$. Elastic parameters of the first part of the composite tube were chosen as those of PDMS, $\rho_w = 987\,\text{kg/m}^3$, $E = 3.6 \times 10^5$ Pa, and $\nu = 0.5$, and those of the second part of the composite tube were chosen as those of PMMA, $\rho_w = 1200\,\text{kg/m}^3$, $E = 3.8 \times 10^9$ Pa, and $\nu = 0.36$. Radius and tube wall thickness were chosen as $a = 1 \times 10^{-4}$ m and $h = 1 \times 10^{-5}$ m. We have verified that the value of $\kappa a < 5 \times 10^{-2}$ for PDMS and $\kappa a < 5 \times 10^{-4}$ for PMMA in the frequency range of panel (a), showing that the example used in this proof of concept is within the range of parameters in which our approximation is valid.

For a zero pressure at the system's outlet, $\Delta\hat{p} = \hat{p}_{\text{out}} - \hat{p}_{\text{in}} = -\hat{p}_{\text{in}}$, and the average flow for the composite tube can be written as

$$\langle \hat{Q}_{\text{composite}} \rangle_x = -\frac{\mathbb{A} K_{\text{composite}}}{\mu(l_1 + l_2)} \Delta\hat{p}, \tag{24}$$

with

$$K_{\text{composite}} = K_1 - (K_1 - K_2)\frac{\hat{p}_J}{\hat{p}_{\text{in}}}, \tag{25}$$

where

$$\frac{\hat{p}_J}{\hat{p}_{\text{in}}} = \frac{K_1 \kappa_1 \sin(\kappa_2 l_2)}{K_1 \kappa_1 \sin(\kappa_2 l_2)\cos(\kappa_1 l_1) + K_2 \kappa_2 \sin(\kappa_1 l_1)\cos(\kappa_2 l_2)}. \tag{26}$$

For this example, the response function, $K_{\text{composite}}$, is explicitly independent from the pressure at the inlet; this can been seen in the right-hand side of Eq. (26) that should be substituted in Eq. (25) and that does not depend on $\hat{p}_{\text{in}}$. It is straightforward to prove that for constant $p_{\text{out}}(t)$, $K_{\text{composite}}$ is also independent of the pressure drop.

Figure 6(a) shows (in orange [light] dashed line) the dynamic permeability for the fluid in a composite tube consisting of two different materials, in which the first third of the tube has the elastic properties of PDMS and the last two thirds of the tube have the elastic properties of PMMA. We have chosen a fluid with the rheological characteristics of blood approximated as a Maxwell fluid. As reference, we also show the permeabilities of the same fluid in both a PDMS tube (in blue [dark] solid line) and a PMMA tube (in green [light] solid line). We have chosen zero pressure at the outlet. Figure 6(b) shows the longitudinally averaged flow, as a function of time, for the three systems of Fig. 6(a) (with the same color coding) when the fluids are driven with a pressure drop $\Delta p(t) = -\Delta p_0 \cos(\omega_0 t)$, with $\omega_0 = 2800$ rad/s and $\Delta p_0 = 20\,\text{Pa}$. The two figures clearly

show what Eq. (24) implies, namely, the magnitude of the dynamic permeability at the driving frequency determines the amplitude of the average flow. That is, by looking at the value of the dynamic permeability of the three systems in Fig. 6(a), at the driving frequency, ω_0, in increasing value (PDMS, composite, and PMMA), we can know that the amplitude of flow will increase in the same order, as illustrated in Fig. 6(b). It is worth noticing that other frequencies will give different results. Driving the same fluid in the same three tubes at $\omega_0 = 5000\,\frac{\text{rad}}{s}$, with all the other parameters as in Fig. 6(b), will cause the amplitude of flow in the composite tube to be the smallest one of the three systems.

Figure 6(a) for the dynamic permeability shows that the zero-frequency response is almost identical for the three systems presented in the graphs. We can therefore know that if we wanted to drive the systems adding a constant pressure drop to the one-mode pressure drop, with frequency ω_0 of the previous example, the steady component of the flow would only translate upward [Fig. 6(b)] by a constant amount, proportional to the dynamic permeability at zero frequency and the constant pressure drop. In this case, flow as a function of time will oscillate around a nonzero mean flow.

VI. CONCLUSIONS AND DISCUSSION

We have analyzed the dynamic permeability of viscoelastic fluids flowing in elastic tubes subject to pulsatile forcing. The dynamic permeability is a frequency-dependent response function characteristic of the fluid-confining-media system. For a given pressure gradient, this response function is linearly related to the amplitude of the average flow along the moving direction. Elasticity on both the fluid and the tube causes the system to have a behavior similar to the one of two coupled oscillators. We have found resonances that can roughly be associated to the elasticity of the tube and resonances that can roughly be associated to the elasticity of the fluid. There is a rich phenomenology that includes cooperation and competition of both elasticities. Tuning the system parameters allows for excitation of the different modes in the system, sometimes giving responses that are larger than the ones of the reference systems with elasticity in only one of its elements, namely the fluid or the confining media, and sometimes permeabilities that are smaller than in those reference systems or intermediate between them.

At very large radii, all resonances are lost, just as has been observed in viscoelastic fluids in rigid tubes [3,5] and in Newtonian fluids in elastomeric tubes [12]. This is because the steady-state permeability grows quadratically with system size and hinders all resonances for large radii.

We also observe that the permeability of a system with elasticity in one of its elements or in both, is always larger (or equal) than the dynamic permeability of a Newtonian fluid in a rigid tube.

The Maxwell model is the simplest model for fluid viscoelasticity. It is almost exact for some systems, like wormlike micelles. Nevertheless, since it involves only one relaxation time, it is often used as an approximation in the literature for many other fluids. However, there are many models for fluid viscoelasticity with different number of relaxation times involved, according to the degree of complexity necessary to describe a particular system. For all models of linear viscoelasticity, resonances exist for viscoelastic fluids in rigid tubes (or cells). See, for example, Ref. [22]. So, we expect our results for Maxwellian fluids in elastic tubes to qualitatively hold for other viscoelastic fluids, since, as we are reporting, the resonance "due to the fluid viscoelasticity" (originally found in rigid systems) is present when the confining media is elastic. This, in principle, should not change qualitatively if the resonances due to the fluid viscoelasticity coming from another model for the fluid.

Our results are potentially useful for tailoring composite laboratory-on-a-chip devices, where changing the elasticity of different parts of a device, by the introduction of different materials, would induce an increase or decrease of the amplitude of the longitudinally averaged flow, at a given frequency, relative to the ones of the tubes made of a single material. As a proof of concept, we analyze flow in a theoretical composite device made of PDMS and PMMA and show that the magnitude of the dynamic permeability for a composite tube, determines the amplitude of the

longitudinally averaged flow. Furthermore, depending on the driving frequency, flow can be larger or smaller than in the homogeneous tubes for an identical amplitude of the driving force.

ACKNOWLEDGMENTS

A.M.T.R. acknowledges financial support from CONACyT (Mexico) through Fellowship No. 245675. E.C.P. declares that the research leading to these results has received funding from the European Union Seventh Framework Programme (FP7-PEOPLE-2011-IIF) under Grant Agreement No. 301214. E.C.P. and A.M.T.R. acknowledge financial support from CONACyT (Mexico) through Project No. 219584, and the Faculty of Chemistry, UNAM, through PAIP Project No. 5000-9011. E.C.P. is grateful to Professor Kerem Uguz and the Department of Chemical Engineering of Bogazici University for hosting her during a sabbatical leave.

APPENDIX: DIMENSIONLESS EQUATIONS

In order to identify characteristic frequencies of the system, we write Eqs. (1)–(5) in a nondimensional form using the following dimensionless quantities:

$$\bar{x} = \frac{x}{a}, \quad \bar{r} = \frac{r}{a}, \quad \bar{t} = \omega_\mu\, t,$$

$$\bar{u} = \frac{u}{a\,\omega_\mu}, \quad \bar{v} = \frac{v}{a\,\omega_\mu}, \quad \bar{p} = \frac{p}{\mu\,\omega_\mu},$$

$$\bar{\eta} = \frac{\eta}{a}, \quad \text{and} \quad \bar{\xi} = \frac{\xi}{a}.$$

where $\omega_\mu = 2\pi \frac{\mu}{\rho\, a^2}$ is the viscous frequency, characteristic of the viscous fluid.

For the continuity equation, we have

$$\frac{\partial \bar{u}}{\partial \bar{x}} + \frac{1}{\bar{r}}\,\frac{\partial(\bar{r}\bar{v})}{\partial \bar{r}} = 0. \tag{A1}$$

The momentum conservation equation is given by

$$\frac{\omega_\mu}{\omega_{t_r}}\,\frac{\partial^2 \bar{u}}{\partial \bar{t}^2} + \frac{\partial \bar{u}}{\partial \bar{t}} = -\frac{\omega_\mu}{\omega_{t_r}}\,\frac{\partial}{\partial \bar{t}}\,\frac{\partial \bar{p}}{\partial \bar{x}} - \frac{\partial \bar{p}}{\partial \bar{x}} + \left(\frac{\partial^2 \bar{u}}{\partial \bar{r}^2} + \frac{1}{\bar{r}}\,\frac{\partial \bar{u}}{\partial \bar{r}}\right), \tag{A2}$$

where $\omega_{t_r} = 2\pi \frac{1}{t_r}$ is given by the inverse relaxation time of the viscoelastic fluid. Note that the dimensionless ratio $\frac{\omega_\mu}{\omega_{t_r}}$ is the inverse Deborah number, α, usually defined for viscoelastic fluids. When the relaxation time is zero, $\alpha^{-1} = 0$, the conservation momentum equation of Navier-Stokes is recovered.

For the radial and axial displacements, we have

$$\frac{\omega_\mu^2}{\omega_e^2}\,\frac{\partial^2 \bar{\eta}}{\partial \bar{t}^2} = \frac{\omega_w\,\omega_\mu}{\omega_e^2}\,\bar{p} - \left(\bar{\eta} + \nu\,\frac{\partial \bar{\xi}}{\partial \bar{x}}\right) \tag{A3}$$

and

$$\frac{\omega_\mu^3}{\omega_{t_r}\omega_e^2}\,\frac{\partial^3 \bar{\xi}}{\partial \bar{t}^3} + \frac{\omega_\mu^2}{\omega_e^2}\,\frac{\partial^2 \bar{\xi}}{\partial \bar{t}^2} = -\frac{\omega_w\,\omega_\mu}{\omega_e^2}\,\frac{\partial \bar{u}}{\partial \bar{r}}\bigg|_a + \frac{\omega_\mu}{\omega_{t_r}}\left(\frac{\partial^3 \bar{\xi}}{\partial \bar{t}\,\partial \bar{x}^2} + \nu\,\frac{\partial^2 \bar{\eta}}{\partial \bar{t}\,\partial \bar{x}}\right) + \left(\frac{\partial^2 \bar{\xi}}{\partial \bar{x}^2} + \nu\,\frac{\partial \bar{\eta}}{\partial \bar{x}}\right), \tag{A4}$$

where $\omega_e = 2\pi \frac{1}{a}\sqrt{\frac{E}{(1-\nu^2)\rho_w}}$ and $\omega_w = 2\pi \frac{\mu}{\rho_w\, h\, a}$. These are two other characteristic frequencies of the system: a characteristic frequency of the elastic wall, ω_e, and a viscous frequency coupled to the tube geometry through the wall thickness and the density of the wall, ω_w. There are two terms

containing the ratio $\frac{\omega_\mu}{\omega_{tr}}$, which come from the viscoelastic nature of the fluid. When these terms are zero, $\alpha^{-1} = 0$ and the equation for the axial deformation of a Newtonian fluid is recovered.

The dimensionless boundary conditions are given by

$$\frac{\partial \bar{\eta}}{\partial \bar{t}} = \bar{v}\Big|_a; \ \frac{\partial \bar{\xi}}{\partial \bar{t}} = \bar{u}\Big|_a. \tag{A5}$$

We solve these equations in Fourier domain following the same methodology presented in Appendix A of Ref. [12] and described in the model equations section of this work.

From the average of the dimensionless axial velocity over the cross-sectional area, $\langle \hat{\bar{u}}(\bar{x}, \bar{\omega}) \rangle$, we can obtain a generalized Darcy's law in terms of the dimensionless pressure gradient in frequency domain, $\bar{g}'(\bar{x})\,\hat{\bar{G}}$, namely

$$\langle \hat{\bar{u}}(\bar{x}, \bar{\omega}) \rangle = -\hat{\bar{K}}(\bar{\omega})\,\bar{g}'(\bar{x})\,\hat{\bar{G}}, \tag{A6}$$

where the frequency is rescaled by the viscous frequency as $\bar{\omega} = \frac{\omega}{\omega_\mu}$. We can define a dimensionless dynamic permeability, $\hat{\bar{K}}(\bar{\omega})$,

$$\hat{\bar{K}}(\bar{\omega}) = \left[\bar{A}\,\frac{2\,J_1(\bar{\delta})}{\bar{\delta}} - \frac{1}{\bar{\beta}^2}\right], \tag{A7}$$

where $\bar{\delta}^2 = \alpha^{-1}\bar{\omega}^2 + i\bar{\omega}$ and $\bar{\beta}^2 = i\bar{\omega}$.

[1] M.-Y. Zhou and P. Sheng, First-principles calculations of dynamic permeability in porous media, Phys. Rev. B **39**, 12027 (1989).

[2] M. L. de Haro, J. A. P. del Río, and S. Whitaker, Flow of Maxwell fluids in porous media, Tran. Porous Med. **25**, 167 (1996).

[3] J. A. del Río, M. L. de Haro, and S. Whitaker, Enhancement in the dynamic response of a viscoelastic fluid flowing in a tube, Phys. Rev. E **58**, 6323 (1998).

[4] J. R. Castrejón-Pita, J. A. del Río, A. A. Castrejón-Pita, and G. Huelsz, Experimental observation of dramatic differences in the dynamic response of Newtonian and Maxwellian fluids, Phys. Rev. E **68**, 046301 (2003).

[5] R. Collepardo-Guevara and E. Corvera Poiré, Controlling viscoelastic flow by tuning frequency during occlusions, Phys. Rev. E **76**, 026301 (2007).

[6] M. Castro, M. E. Bravo-Gutiérrez, A. Hernández-Machado, and E. C. Poiré, Dynamic Characterization of Permeabilities and Flows in Microchannels, Phys. Rev. Lett. **101**, 224501 (2008).

[7] G. B. Thurston and N. M. Henderson, Effects of flow geometry on blood viscoelasticity, Biorheology **43**, 6 (2006).

[8] Y. Majima, T. Harada, T. Shimizu, K. Takeuchi, Y. Sakakura, S. Yasuoka, and S. Yoshinaga, Effect of biochemical components on rheologic properties of nasal mucus in chronic sinusitis, Am. J. Resp. Crit. Care **160**, 421 (1999).

[9] P. Tabeling and S. Chen, *Introduction to Microfluidics* (Oxford University Press, Oxford, UK, 2005).

[10] D. S. Kim, S. H. Lee, C. H. Ahn, J. Y. Lee, and T. H. Kwon, Disposable integrated microfluidic biochip for blood typing by plastic microinjection moulding, Lab Chip **6**, 794 (2006).

[11] S. Yang, A. Ündar, and J. D. Zahn, A microfluidic device for continuous, real time blood plasma separation, Lab Chip **6**, 871 (2006).

[12] A. M. Torres Rojas, I. Pagonabarraga, and E. Corvera Poire, Resonances of Newtonian fluids in elastomeric microtubes, Phys. Fluids **29**, 122003 (2017).

[13] D. Tsiklauri and I. Beresnev, Enhancement in the dynamic response of a viscoelastic fluid flowing through a longitudinally vibrating tube, Phys. Rev. E **63**, 046304 (2001).

[14] D. Tsiklauri and I. Beresnev, Properties of elastic waves in a non-Newtonian (Maxwell) fluid-saturated porous medium, Tran. Porous Med. **53**, 39 (2003).

[15] D. Tsiklauri and I. Beresnev, Non-Newtonian effects in the peristaltic flow of a Maxwell fluid, Phys. Rev. E **64**, 036303 (2001).

[16] M. Zamir, *The Physics of Pulsatile Flow* (Springer, New York, 2000).

[17] J. Mazumdar, *An Introduction to Mathematical Physiology and Biology* (Cambridge University Press, Cambridge, UK, 1999).

[18] The solution of the system of Eqs. (1)–(5), gives analytical expressions for the radial velocity, $\hat{v}$, and the radial and axial displacements, $\hat{\eta}$ and $\hat{\xi}$. However, it is important to note that such quantities are not independent of the axial velocity, $\hat{u}$. Our analysis therefore focuses on the dynamic response of the axial velocity.

[19] It is worth noticing that Eqs. (6)–(14) are in frequency domain, that is, the variable frequency, ω, is not a driving frequency, ω_0. This is very different from other works in the literature done for traveling waves in which a one-mode dependence is proposed for all the variables in the system in order to get a solution.

[20] Equivalent treatments can be made for any number of modes. For example, for an n-mode pressure drop $\Delta p(t) = -\Delta p_1 \cos(\omega_1 t) - \Delta p_2 \cos(\omega_2 t) - \cdots - \Delta p_n \cos(\omega_n t)$ we would obtain an equivalent Eq. (15) as $\langle Q(t)\rangle_x = \frac{\mathbb{A}}{\mu}|\hat{K}(\omega_1)|\cos[\phi(\omega_1) - \omega_1 t]\frac{\Delta p_1}{l} + \frac{\mathbb{A}}{\mu}|\hat{K}(\omega_2)|\cos[\phi(\omega_2) - \omega_2 t]\frac{\Delta p_2}{l} + \cdots + \frac{\mathbb{A}}{\mu}|\hat{K}(\omega_n)|\cos[\phi(\omega_n) - \omega_n t]\frac{\Delta p_n}{l}$, where $|\hat{K}(\omega_i)|$ and $\phi(\omega_i)$ are the magnitude and phase of the dynamic permeability at the frequency ω_i. In particular, if one of the modes were a zero-frequency mode, which would correspond to a constant pressure drop, Δp_{const}, we would obtain a steady component of the flow, given by $\langle Q_{ss}\rangle_x = \frac{\mathbb{A}\Delta p_{\text{const}}}{\mu l}|\hat{K}(0)|$.

[21] J. Flores, E. C. Poiré, J. Del Río, and M. L. de Haro, A plausible explanation for heart rates in mammals, J. Theor. Biol. **265**, 599 (2010).

[22] M. E. Bravo-Gutiérrez, M. Castro, A. Hernández-Machado, and E. Corvera Poiré, Controlling viscoelastic flow in microchannels with slip, Langmuir **27**, 2075 (2011).